Mechanical, Thermal, and Microwave Properties of Conducting Composites of Polypyrrole/Polypyrrole-Coated Short Nylon Fibers with Acrylonitrile Butadiene Rubber

D. S. Pramila Devi, Ajalesh. B. Nair, T. Jabin, Sunil K. N. Kutty

Department of Polymer Science and Rubber Technology, Cochin university of Science and Technology, Cochin, India

Received 25 November 2011; accepted 31 January 2012
DOI 10.1002/app.36924
Published online in Wiley Online Library (wileyonlinelibrary.com).

ABSTRACT: Pyrrole was polymerized in the presence of anhydrous ferric chloride as oxidant and *p*-toluene sulfonic acid as dopant. Polypyrrole-coated short nylon fibers were prepared by polymerizing pyrrole in the presence of short nylon fibers. The resultant polypyrrole (PPy) and PPy-coated nylon fiber (F-PPy) were then used to prepare rubber composites based on acrylonitrile butadiene rubber (NBR). The cure pattern, direct current (DC) conductivity, mechanical properties, morphology, thermal degradation parameters, and microwave characteristics of the resulting composites were studied. PPy retarded the cure reaction while F-PPy accelerated the cure reaction. Compared to PPy, F-PPy was found to be more effective in enhancing the DC conductivity of NBR. The tensile strength and modulus values increased on adding PPy and F-PPy to NBR, suggesting a reinforcement effect. Incorporation of PPy and F-PPy improved the thermal stability of NBR. The absolute value of the dielectric permittivity, alternating current (AC) conductivity, and absorption coefficient of the conducting composites prepared were found to be much greater than the gum vulcanizate. PPy and F-PPy were found to decrease the dielectric heating coefficient and skin depth significantly. © 2012 Wiley Periodicals, Inc. J Appl Polym Sci 000: 000–000, 2012

Key words: polypyrrole; rubber; nylon; composites

INTRODUCTION

The conducting polymers constitute a family of organic conductors whose electric and mechanical properties are studied since the end of 1970. Research in the field of such polymers aims mainly at some suitable modifications of existing polymers so that their applicability can be improved. In this family, one finds composite materials obtained from the dispersion of a conducting polymer in an insulating matrix. These composites are increasingly required in industry for their great potentialities of applications in various fields. The incorporation of conductive particles (carbon black, metal, etc.) into a polymer matrix modifies considerably the electrical conductivity of the composite,[1–3] but the presence of this type of load deteriorates considerably the mechanical characteristics of the composites compared with those of noncharged materials. The use of conducting polymers made it possible to obtain composites having at the same time a raised electric conductivity associated with good mechanical properties.[4] These materials have the effect of combining electric properties, of conducting polymers with the mechanical properties of the plastics.[5] Evaluation of magnetic and dielectric properties of the composites and correlation of results may help in tailoring composites for electronic and electrical applications such as electrostatic charge dissipation, touch control switches, electromagnetic interference shielding, pressure sensor, etc.[6–8] Evaluation of AC electrical conductivity reveals a wealth of information on the usefulness of these materials for various applications. Moreover the study of AC electrical conductivity sheds light on the behavior of charge carriers under an AC field, their mobility and the mechanism of conduction.[9–11]

Among the conducting polymers, polypyrrole (PPy) is one of the most studied one because of its high electrical conductivity, environmental stability, and ease of synthesis.[12] However, as any other conjugated conducting polymer, PPy lacks processability, flexibility, and strength. This can be improved either by forming copolymers of PPy or by forming PPy composites or blends with suitable, commercially available polymers. Composites of PPy with many polymers such as polymethylmethacrylate, poly(vinyl carboxyethylether), polyethylene terephthalate (PET) fabrics, natural and synthetic rubbers, chlorinated polyethylene have been reported.[13–17] Even though all these composites exhibit excellent conducting and shielding properties, the main concern with most of them is the lack of good mechanical properties. To couple these two properties, special materials have to be developed. If PPy is

Correspondence to: S. K. N. Kutty (sunil@cusat.ac.in).

adhered to a strong substrate and then used as a filler in polymer matrix, improvement in mechanical properties is expected.[18] The electrical and mechanical properties of polymer blends/composites depend on the aspect ratio of the additive. Conducting polymers are usually spherical in shape, with small aspect ratio. But, fibers are characterized by high aspect ratios. It is well established that mechanical properties of rubber composites can be greatly improved by adding short fibers.[19] Generally, short fiber reinforced rubber composites are popular in industrial fields because of their processing advantages, low cost, and their greatly improved technical properties such as strength, stiffness, modulus, and damping.[20] Hence, conducting fibers used as additives can impart good mechanical properties along with desirable electrical properties. Elastomeric conducting composites of polyaniline-coated short nylon fiber with natural rubber and chloropene rubber were prepared and the mechanical, thermal, and microwave characteristics were studied by Chandran.[21]

In this work, an attempt has been made to prepare a conducting composite with reasonable conductivity along with good mechanical properties. A conducting composite using PPy and acrylonitrile butadiene rubber (NBR) is prepared. NBR has good resistance to a wide variety of oils and solvents and hence is widely used in products such as oil seals, pipe protectors, blow-out preventors. The use of PPy-coated fiber is expected to improve the mechanical properties of the NBR-PPy composite, while increasing the conductivity. The thermal and microwave properties of the prepared composites are also investigated.

EXPERIMENTAL

Materials

Nylon-6 fiber was obtained from SRF, Chennai, India. Pyrrole and *p*-toluene sulfonic acid were supplied by Spectrochem, Mumbai. Anhydrous Iron(III) chloride was obtained from Merck Specialities, Mumbai. NBR was supplied by Kumho Petrochemicals, Korea. Zinc oxide, stearic acid, tetramethylthiuram disulfide (TMTD), mercaptobenzothiazyl disulfide (MBTS), and sulfur used were of commercial grade. Pyrrole monomer was purified by distillation and stored at 4°C in the absence of light.

Preparation of polypyrrole

PPy was prepared by chemical oxidative polymerization of pyrrole using anhydrous ferric chloride as oxidant and *p*-toluene sulfonic acid as dopant in aqueous medium. Molar ratio of oxidant to monomer was 2.22 and dopant to monomer ratio was 0.4. The reaction was carried out at 4°C with continuous stirring for 4 h. Precipitated PPy was filtered, washed with water till the filtrate became colorless, followed by a wash with methanol to remove unreacted pyrrole, and then dried in air oven at 55°C for 24 h.

TABLE I
Formulation of Composites

Sample	PPy (phr)[a]	F-PPy (phr)
BP0	0	0
BP1	20	0
BP2	50	0
BP3	75	0
BP4	100	0
BFp1	0	10
BFp2	0	25
BFp3	0	50
BFp4	0	75

All mixtures contain NR 100 g, zinc oxide 4.5 phr, stearic acid 2 phr, tetramethylthiuram disulfide 0.25 phr, mercaptobenzothiazyl disulfide 1 phr, and sulfur 1.5 phr.
[a] Parts per hundred rubber.

Preparation of PPy-coated fiber

Nylon-6 fibers, chopped to 6 mm length, were soaked in pyrrole for 1 h and subjected to in situ polymerization of pyrrole using anhydrous ferric chloride as oxidant and *p*-toluene sulfonic acid as dopant in aqueous medium to get PPy-coated short nylon fibers (F-PPy).The coated fibers were then filtered, washed with water till the filtrate became colorless, followed by a wash with methanol to remove unreacted pyrrole, and then dried in air oven at 55°C for 24 h.

Composite preparation

The formulation for the preparation of composites is given in Table I. The composites were prepared in a laboratory size (15 × 33 cm) two-roll mill at a friction ratio of 1 : 1.25 as per ASTM D 3184 (1980). BP series represents the vulcanizates of NBR with PPy and BFp represents NBR/F-PPy composites. The mixtures were then passed through a tight nip to prepare thins sheets with fibers oriented in the mill direction. The sheets were kept for 24 h for maturation. The optimum cure time at 160°C was determined using a rubber process analyzer. The compounds were compression molded at 160°C in an electrically heated hydraulic press having 30 × 30 cm^2 platens at a pressure of 200 kg cm^{-2} into sheets using standard mold (15 × 15 × 2 cm^3). The rubber compounds were vulcanized to their respective cure times. After curing, the pressure was released, and

the sheets were stripped off from the mold and cooled suddenly by plunging into water. These sheets were used for subsequent tests.

Fourier transform infrared spectroscopy

Fourier transform infrared spectroscopy spectrum of PPy was taken using Thermo Nicolet Avatar 370 having spectral range of 4000–400 cm^{-1} and a resolution of 0.9 cm^{-1} and equipped with KBr beam splitter and DTGS Detector.

Cure characteristics

The cure characteristics of the vulcanizates were determined using a Rubber Process Analyzer (RPA 2000, Alpha Technologies) as per ASTM D 2084-01. A biconical die with a die gap of 0.487 mm was used. The cure time T_{90}, scorch time T_{10}, maximum torque M_H, and minimum torque M_L values were determined at 160°C at a frequency of 50.0 cpm and a rotational amplitude of 0.2°.

Scanning electron microscopy

Scanning electron microscopic (SEM) images of PPy, virgin nylon-6 fiber , F-PPy, and the composites were obtained using a Cambridge Instruments S 360 stereo scanner-versionV02-01.

DC electrical conductivity

The DC electrical conductivity of the composites was measured by the two-probe method using a Keithley2400 source-measure unit.

Mechanical properties

The stress–strain behavior of the composites were studied using a Shimadzu Universal Testing Machine (model AG-I) with a load cell of 10 kN capacity at a crosshead speed of 500 mm min^{-1} and at a gauge length of 40 mm. The measurements were carried out as per ASTM D 412-98a (2002). Dumbbell-shaped samples were punched out from the compression molded sheets along the mill grain direction. Tear strength of the samples were measured as per ASTM D 624-2000 using standard test specimens (Type C die) which were punched out from the compression molded sheets along the mill grain direction.

Thermogravimetric analysis

Thermogravimetric studies were performed on a Q 20, TA Instruments thermogravimetric analyzer (TGA) with a programmed heating of 20°C min^{-1} from room temperature to 800°C. The chamber was continuously swept with nitrogen at a rate of 90 mL min^{-1}. The temperature at maximum degradation was taken as the peak degradation temperature and the rate of degradation at the peak degradation temperature was recorded as the peak degradation rate. The weight percentage of the samples remaining at 800°C was recorded as the residue.

Microwave properties

The microwave characteristics of the prepared conducting polymer composites were studied using cavity perturbation technique.[22–26] The experimental set up consists of a ZVB20 vector network analyzer; sweep oscillator, *S*-parameter test set, and rectangular cavity resonator. The measurements were done in *S* (2–4 GHz) band frequencies at room temperature (25°C). The dimensions of *S*-band rectangular wave-guide used in the measurements are 34.5 × 7.2 × 3.4 cm^3.

The quality factor, Q_0, of the cavity and resonance frequency, $f_{0,}$ in the unperturbed conditions were measured. The samples in the form of thin rectangular roads, the length of which equals the height of the cavity so that both the ends of the specimen are in contact with the cavity walls, were used. The samples were inserted into the cavity through a slot and positioned at the maximum electric field. The resonance frequency, $f_{s,}$ and loaded quality factor, $Q_{s,}$ of the samples were measured. Knowing the volume of cavity, V_c, and volume of sample, V_s, the dielectric permittivity and dielectric loss were calculated. All other microwave characteristics of the composites can be determined from these permittivity values.

$$\text{Dielectric permittivity, } \varepsilon' = 1 + (f_0 - f_s)/2f_s.(V_c/V_s)$$

$$\text{Dielectric loss, } \varepsilon'' = (V_c/4V_s)[(Q_o - Q_s)/Q_oQ_s]$$

$$\text{Loss tangent, } \tan\ \delta = \varepsilon''/\varepsilon'$$

$$\text{AC conductivity, } \sigma = \omega\varepsilon'' = 2\Pi f_s\, \varepsilon_0\, \varepsilon''$$

where ε_0 is the complex permittivity of the free space.

$$\text{Dielectric heating coefficient, } J = 1/\varepsilon * \tan\delta$$

where ε* is the relative complex permittivity of the sample material

$$\text{Absorption coefficient, } \alpha_f = \varepsilon'' f_s/nc$$

where $n = \varepsilon^*$ and "c" is the velocity of light.

$$\text{Skin depth, } \delta_f = 1/\alpha_f$$

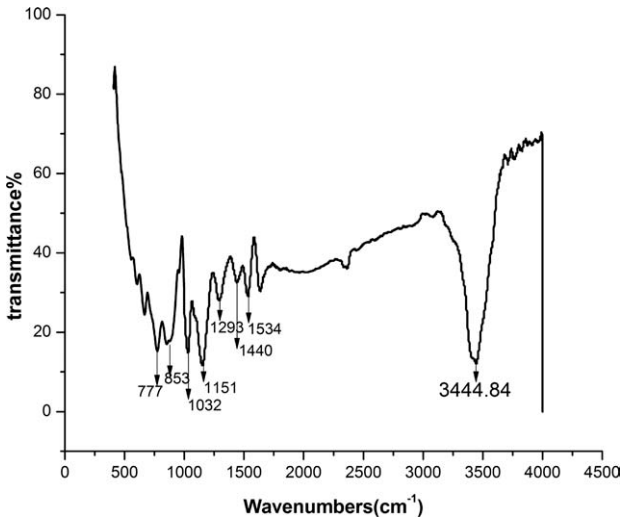

Figure 1 IR spectrum of polypyrrole.

RESULTS AND DISCUSSION

IR spectroscopy

Figure 1 shows the IR spectrum of PPy. The IR peak obtained at 3444 cm^{-1} is due to N—H stretching.[27] The band at 1534 cm^{-1} corresponds to C=C stretching and that at 1440 cm^{-1} to C—C and C—N stretching: i.e., typical PPy ring vibrations. The peak at 1293 cm^{-1} may be assigned to mixed bending and stretching vibrations associated with C—N links.[28,29] C=N stretching gives a band at 1151 cm^{-1}. In-plane deformation vibrations of C—H bond and N—H bond of pyrrole ring give rise to a peak at 1032 cm^{-1}.[30] IR peak at 853 cm^{-1} is due to C=H out-of-plane vibration indicating polymerization of pyrrole.[31] The band at 777 cm^{-1} may be assigned to N—H out-of-plane vibration.[32]

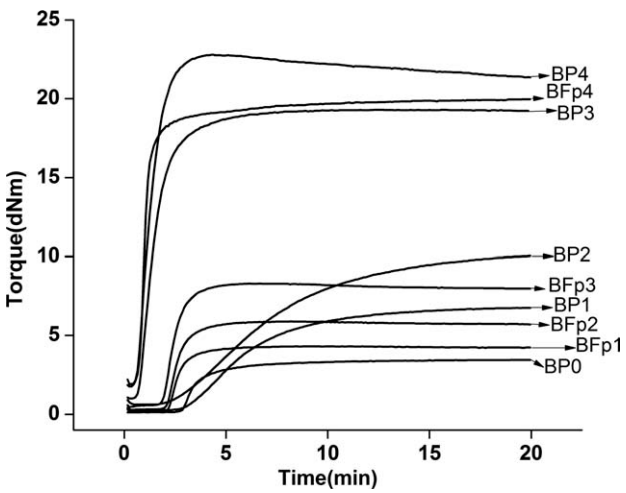

Figure 2 Cure curves of the composites.

TABLE II
Cure Parameters of Composites

Sample	Cure time T_{90} (min)	Scorch time T_{10} (min)	Maximum torque M_H (dNm)	Minimum torque M_L (dNm)
BP0	6.5	2.9	3.5	0.1
BP1	10.9	3.5	6.8	0.2
BP2	13.2	3.2	10.0	0.6
BP3	3.0	0.8	19.3	1.0
BP4	2.2	0.7	22.8	1.9
BFp1	3.8	2.2	4.3	0.1
BFp2	3.8	2.2	5.9	0.3
BFp3	3.4	1.9	8.3	0.4
BFp4	1.9	0.7	19.9	1.7

Cure characteristics

Figure 2 shows the cure curves of the composites. The nature of the cure curves is different for the series, which indicates that in the matrix, PPy and F-PPy interact differently. The cure parameters of the composites are presented in Table II. Cure time, $T_{90,}$ represents the time corresponding to the development of 90% of the maximum torque. Cure time is found to increase with the incorporation of PPy, reaches a maximum and then found to decrease at higher loading. The increase in cure time with PPy concentration may be attributed to presence of acidic dopant in PPy. For BFp series, cure time decreases substantially on loading with F-PPy. This may be due to possible degradation of nylon fibers at the curing temperature. The effect of PPy is not manifested here as the PPy content is very low in this case. The amine functionality of the degradation products may accelerate the cure reaction. Similar results have been reported earlier in the cases of natural rubber (NR)/short nylon fiber composites,[33] NBR/short nylon fiber composites[34] and NR/polyaniline/polyaniline-coated short nylon fiber composites.[21]

Scorch time T_{10} is the time required for the torque value to reach 10% of maximum torque. It is a measure of the scorch safety of the rubber compound. For BP series, scorch time increases with filler loading initially indicating a better processing safety. Subsequently, the value decreases. For the BFp series, scorch time is found to decrease with loading. Such a decrease is attributable to the heat of mixing of highly loaded samples, resulting in the premature curing of the compounds. The maximum torque, M_H is an index of the extent of crosslinking reactions and represents the shear modulus of the fully vulcanized rubber at the vulcanization temperature. It is also a measure of the filler–polymer interactions. The value is found to increase for the two series. The minimum torque, M_L, a measure of the viscosity of the compound, is found to increase with filler loading for the two series. The increase in viscosity with the addition

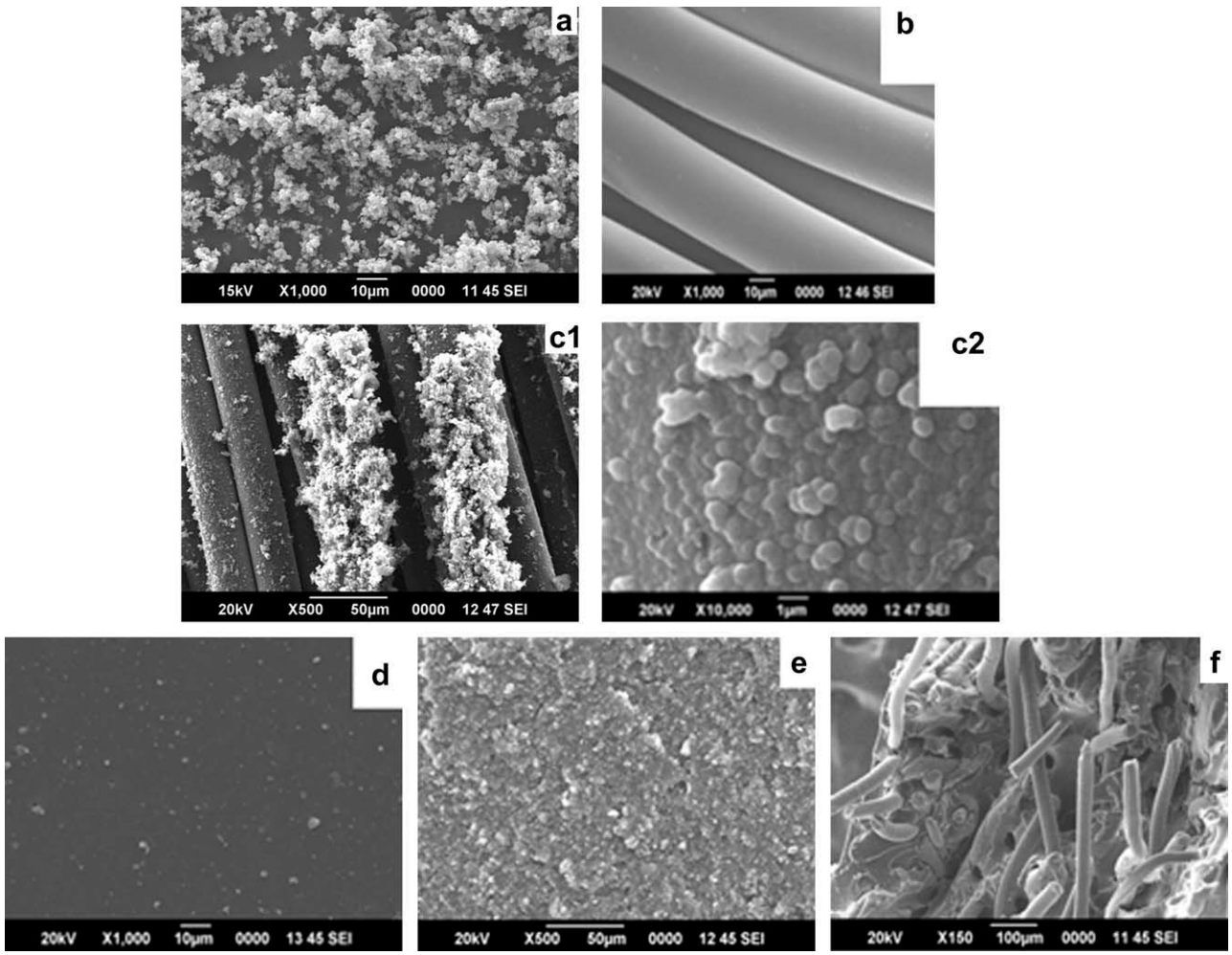

Figure 3 SEM micrographs of (a) PPy, (b) virgin nylon-6, (c1,c2) F-PPy, (d) BP0, (e) BP2, and (f) BFp2.

of filler suggests a reduced mobility of the rubber chains in the presence of these fillers.

Morphology

The SEM micrographs of PPy (a), virgin nylon-6 fiber (b), F-PPy (c1 and c2), and the micrographs of failed tensile surfaces of the composites BP0 (d), BP2 (e), and BFp2 (f) are shown in Figure 3. The granular morphology of PPy powder is visible in Figure 3(a). The powder is composed of quasi-spherical particles with diameter of about 250 nm bonded to each other in irregular agglomerates. Similar morphology for chemically polymerized PPy has been reported.[32,35,36] Figure 3(b) shows the smooth surface of uncoated nylon-6 fiber. Figure 3(c1,c2) show that PPy forms a dense coating of fused small spheres on nylon fiber. Some aggregates of spherical particles are also formed. Similar morphology PPy coated on PET fibers has been reported already.[37,38] PPy-coated cotton, cellulose, and silk fibers with similar morphologies have also been reported.[32,39,40]

Figure 3(d) shows the SEM photograph of the tensile fracture surface of the gum vulcanizate. The fracture surface is smooth and has no crack propagation lines. This pattern is typical of weak matrices. SEM images of PPy/NBR composite [Fig. 3(e)] reveal a homogenous dispersion of PPy in the rubber matrix. The cluster and granular structure of PPy are maintained even in the composite. PPy primary particles link with each other to form conductive chains or network in the NR matrix. Hence, conductivity is expected to increase with filler loading. Murugendrappa et al.[41] have reported such a morphology for PPy/Fly ash composites. SEM studies on PPy/Y_2O_3 composites by Vishnuvardhan et al.[42] also have reported similar observations.

The SEM image of NBR/F-PPy composites, Figure 3(f) shows better adhesion between fiber and matrix and good orientation of fiber in one direction, i.e., longitudinal, resulting in improved mechanical properties, as will be discussed shortly.

DC electrical conductivity

The DC electrical conductivities of the composites are presented in Figure 4. For the BP series, there is

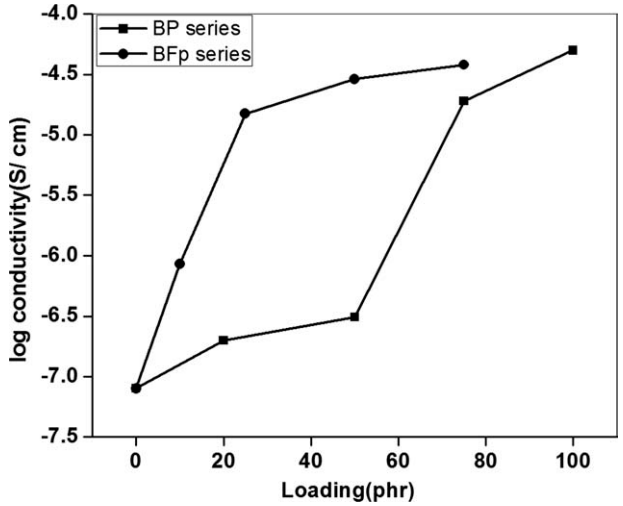

Figure 4 Variation of log conductivity with filler loading.

not much increase in conductivity up to 50 phr loading. After that, a sharp increase in conductivity is observed with a maximum of 5×10^{-5} S cm^{-1}, attained at 100 phr loading. For BFp series, percolation occurs at about 25 phr F-PPy loading and levels off at higher loadings.

Morphology, including the formation of microcells and the dispersion of conducting material in the composite become important factor that determines conductivity.[43] Despite better dispersion of PPy in NBR matrix as is evident from SEM images discussed earlier, one possible reason for the lower percolation threshold in the case of BFp series compared to BP series is the increasing fiber–fiber contact forming a conductive pathway in the matrix. This closed network of conducting species is absent in BP series. The conductivity of a sample has two aspects: microscopic conductivity, which depends on the doping level, conjugation length, chain length, etc., and macroscopic conductivity, which is determined by external factors such as the compactness of the samples. The microscopic conductivity did not vary a lot in our samples because the composites were prepared in an identical manner. However, the macroscopic properties, such as compactness, significantly changed depending on the type of filler in the composite—PPy or F-PPy. Pure PPy is a polymer with poor compactness. PPy particles are very randomly oriented and the linking between the polymer particles through the boundaries is very poor, which results in relatively high percolation threshold of PPy loaded composites. In the NBR/F-PPy composites, the filler is PPy-coated fibers. So the compactness of PPy in the composite is much tighter than pure PPy. Moreover, because of the large aspect ratio and surface area of the fibers and due to the longitudinal orientation of PPy-coated fibers they may serve as effective percolative conducting bridges that increase the conductivity of the composite. Such a phenomenon has been observed by Gu et al.[44] in composites of PPy with graphite oxide.

Mechanical properties

The variation of tensile strength of PPy-loaded (BP series) and F-PPy-loaded (BFp series) samples are shown in Figure 5. The tensile strength of elastomer increases gradually with PPy loading and an increase of 125% is observed at 75 phr loading after which it levels off. This reveals the reinforcing nature of PPy in NBR matrix. Introduction of PPy into a composite, as a rule, decreases its strength and results in the loss of elasticity.[45] Here, the better interaction between PPy and the nitrile rubber matrix is the main factor for the increase of tensile strength. Tensile strength of BFp series shows a marginal increase at 10 phr loading, beyond which a sharp increase is observed and reaches a maximum at 50 phr loading. Presence of F-PPy in the matrix along the longitudinal direction of application of force (as is evident from SEM) are much effective in hindering the growing crack front and requires that greater force be applied to pull out the fiber from the fiber–rubber interface. This results in higher tensile strength in that direction. As fiber concentration increases, there are more and more fibers to hinder the crack front and tensile strength increases. At very high loading, the relative proportion of the matrix is low and the reinforcement becomes ineffective, dilution effect predominates, which tends to decrease the tensile strength as is the case with 75-phr F-PPy-loaded sample. Similar observations in the case of short nylon fiber reinforced elastomer composites have been reported.[21,33,34]

Elongation at break decreases with PPy loading (Fig. 6) as the composites become increasingly stiffer.

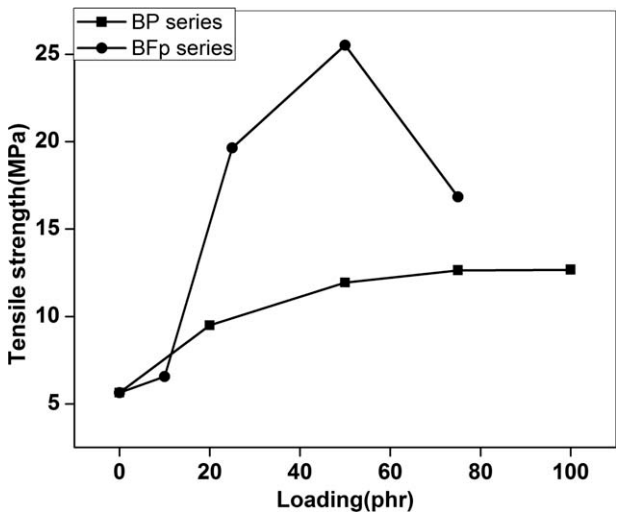

Figure 5 Variation of tensile strength with filler loading.

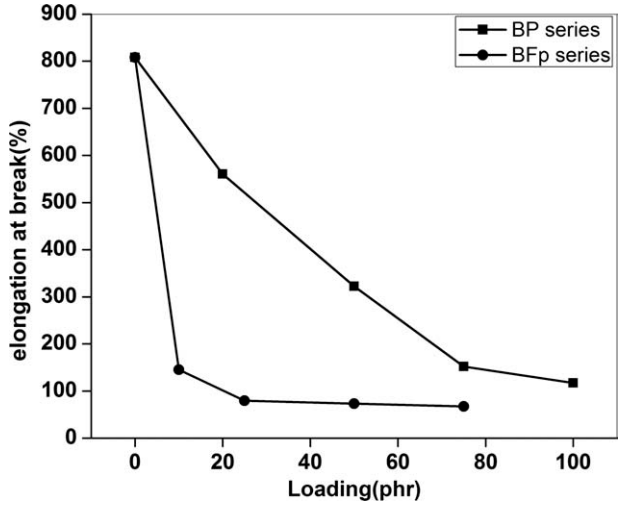

Figure 6 Variation of elongation at break with filler loading.

Figure 6 also shows that the ultimate elongation shows a sharp fall upon the introduction of 10 phr F-PPy, but with further increase, the values tend to stabilize. In the presence of short fibers, the matrix is more restrained, and the failure is initiated at multiple points, resulting in lower ultimate elongation values.

Modulus at 50% elongation increases for the two series (Fig. 7). The variation is same as that of tensile strength. Variation of tear strength with filler loading for BP series and BFp series is shown in Figure 8. Tear strength is found to increase sharply with PPy and F-PPy loading. The fiber-loaded samples exhibit higher values. The tear failure occurs by the propagation of tear front across the matrix. In the presence of fibers distributed in the bulk, these tear lines are either arrested or deviated. The energy of the propagating crack front is dissipated at the

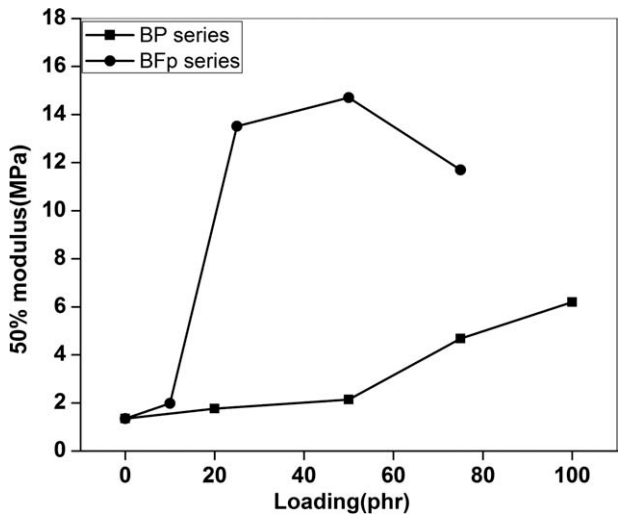

Figure 7 Variation of modulus at 50% elongation with filler loading.

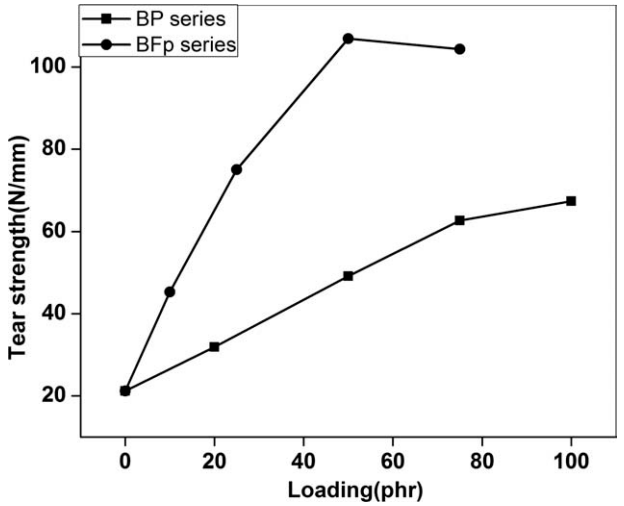

Figure 8 Variation of tear strength with filler loading.

fiber–matrix interface by way of its pull-out or breakage. This results in improved tear resistance.

Thermal properties

The thermal mass loss traces obtained from the TG analysis of pure PPy, BP0, BP2, and BP3 are reported in Figure 9. The TG curves of virgin nylon fiber (Fv), PPy-coated nylon fiber (F-PPy), BP0, BFp2, and BFp4 are presented in Figure 10. Dependence of degradation of the composites on PPy loading and F-PPy loading are better visualized in the DTG curves which are given as inset boxes in Figures 9 and 10, respectively. The thermal characteristics of the composites are presented in Table III. Analysis of TG curves of pure PPy shows a first weight loss of 6.5% which is due to loss of moisture. The second degradation, with a peak degradation

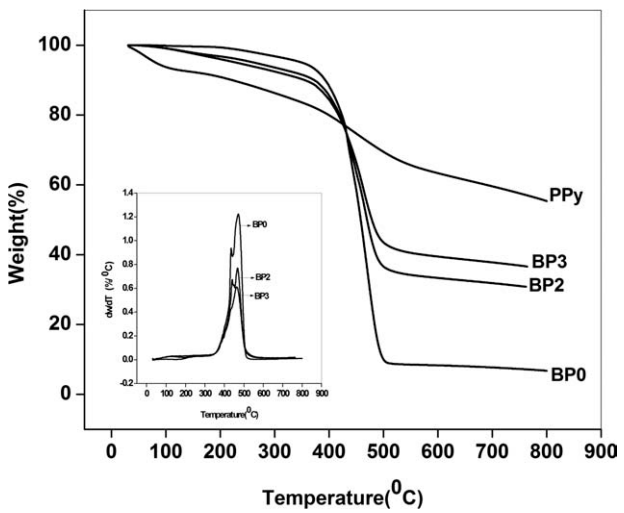

Figure 9 TGA thermograms of pure PPy and composites of BP series. DTG curves of BP series are reported in the inset box.

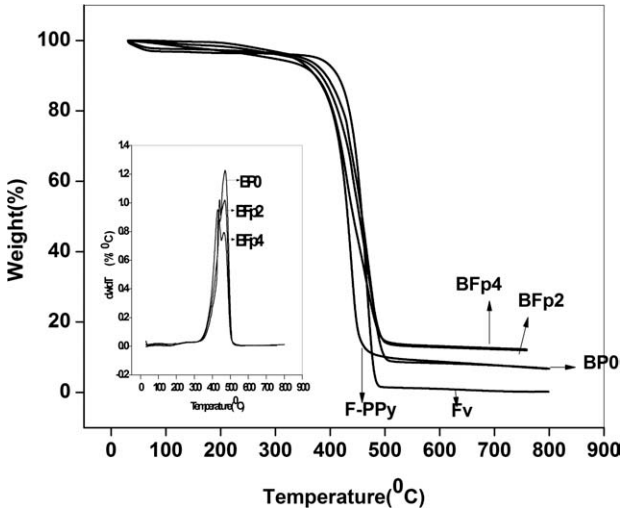

Figure 10 TGA thermograms of virgin nylon fiber (Fv), PPy-coated nylon fiber (F-PPY), and composites of BFp series. DTG curves of BFp series are reported in the inset box.

occurring at 448°C corresponds to degradation of PPy chain. Less than 30% weight loss occurs during this degradation. At 800°C, the residue weight is 55%.This indicates the high thermal stability of PPy which is in good agreement with the report of Cataldo and Omastova[46] that PPy produced with $FeCl_3$ as oxidant has a quite good thermal stability. Similar thermograms for PPy have been reported by others.[44,47]

TG analysis of composites shows that the onset of degradation shifts to higher temperatures on adding PPy to NBR, due to the high thermal stability of PPy. No such change is observed with the addition of F-PPy because onset of degradation of F-PPy is found to be the same as that of NBR gum vulcanizate. First degradation peak is obtained in the range 430–440°C for all composites. The second peak degradation temperature decreases for BP series while it remains almost constant in the case of BFp series. This is due to the fact that peak degradation occurs at 448°C in the case of PPy while for F-PPy, maximum degradation occurs at a still higher temperature, 475°C. The peak degradation rate, i.e., the maximum rate of degradation recorded (at the peak degradation temperature) is found to decrease with filler loading for both series. Lower rate means that the compound will degrade only slowly. This is better understood from the DTG plots. Table III shows that this decrease is more pronounced in the case of BP series, again due to the higher thermal stability of PPy compared to F-PPy. The same trend is observed for weight loss at peak degradation temperature. The sharp decrease in this weight loss on PPy loading compared to F-PPy loading is attributed to the extremely high thermal stability of PPy. The temperature corresponding to 50% weight loss increases for BP series while remains almost same for BFp series. An increased weight loss is observed at 300°C for BP series compared to BFp series. This is due to a weight loss occurring in pure PPy between 67 and 140°C (Fig. 9). Such a weight loss is not expected in the case of BFp series as PPy content coated on fibers is very low. The weight remaining at 600 and 800°C are much higher for PPy loaded samples. All these results ascertain that the thermal stability of the composites increases steadily with PPy and F-PPy loading. According to Gilman,[48] the improvement in thermal stability of polymers in presence of fillers is due to the hindered thermal motion of polymer molecular chain.

Microwave properties

Dielectric permittivity

The variation of dielectric permittivity (ε′) of NBR with PPy loading and F-PPy loading in S-band frequency are shown in Figures 11 and 12, respectively. Higher the polarizability of the material, the greater the dielectric constant. The frequency dependence of dielectric permittivity of these composites can be explained as follows: below frequencies of 10^{10} Hz, all polarization mechanisms—electronic, ionic, and dipolar—contribute to dielectric permittivity. Further, the prepared composites are a heterogenous

TABLE III
Thermal Characteristics of the Composites

Thermal degradation parameters	Sample code						
	Fv	F-PPy	BP0	BP2	BP3	BFp2	BFp4
Onset degradation temperature (°C)	376	338	337	351	348	336	339
Peak degradation temperature (°C)	468	475	1st 434	440	430	443	434
			2nd 476	469	464	474	470
Peak degradation rate of second peak (%/°C)	2.26	2.01	1.181	0.767	0.608	1.016	0.792
Weight loss at peak degradation temperature (%)	94.3	86	88.2	59.4	51.9	83.1	81.4
Temperature at 50% weight loss (°C)	459	437	458	470	477	457	446
Weight remaining at 300°C (%)	96.2	96.4	96.8	93.6	92.4	96.2	94.9
Weight remaining at 600°C (%)	1	8.8	8.3	33.3	39.4	12.8	13.1
Residue at 800°C (%)	0.2	6.7	6.8	30.8	36.6	11.9	12.2

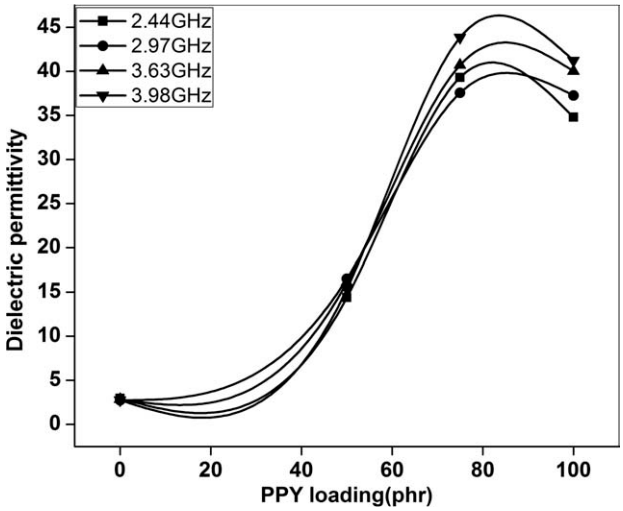

Figure 11 Dielectric permittivity versus PPy loading of BP series.

mixture of conducting PPy separated by highly resistive rubber matrix. The dielectric permittivity of such heterogenous, conducting composites arises mainly due to interfacial polarization along with some contributions from intrinsic electric dipole polarization.[49] Doped PPy possess permanent electric dipoles. Therefore, orientation or dipolar polarization is expected to contribute to the dielectric permittivity. Of these polarization mechanisms, dipolar and interfacial (space charge) are more frequency dependent. It has been shown that ε' is almost constant regardless of applied frequency for BP series especially BPO and BP2. Therefore in these, the polarization mechanisms contributing to ε' may be electronic and ionic. For BP3 and BP4, there is a slight increase in ε' with frequency which can be attributed to the contribution due to increased dipolar polarization arising from increased PPy content. When it comes to BFp series, PPy-coated fibers contribute more conducting regions in the system, leading to increase in space charge polarization which depend more on the frequency of applied field. The observed decrease in ε' with increasing frequency in the case of BFp series may be attributed to the decrease in space-charge polarization with increasing frequency.[50,51] This behavior is in accordance with Maxwell–Wagner interfacial polarization. As the frequency of applied field increases, interfacial polarization decreases and hence dielectric permittivity decreases. As the frequency is increased, the time required for the interfacial charges to be polarized or for the dipoles to be arranged is delayed, thus the dielectric permittivity decreases with frequency.

There is a substantial increase in ε' with PPy loading. The increase in ε' with increasing PPy content may be due to increase of conducting regions. According to Koops, the dielectric permittivity is inversely proportional to the square root of resistivity.[9] The DC conductivity of NBR-based composites increases with loading. A dielectric permittivity of 43 is obtained for 75-phr PPy-loaded composite (BP3) at 3.9 GHz frequency. For a PANI/NR semi-interpenetrating network from NR latex, John et al.[52] have reported a permittivity of 20 at a NR:PANI proportion of 2 : 1. For a PANI/NR composite, Chandran et al.[21] have reported a dielectric permittivity of 35 for 140-phr PANI-loaded sample at 4 GHz frequency. Incorporation of F-PPy causes an increase in ε', reaches maximum at 50 phr loading and then decreases. This is in accordance with DC conductivity values, discussed earlier. At 50-phr F-PPy loading, maximum conductivity is attained. Further loading does not bring about any increase in conducting regions and therefore in space charge polarizability. Thus, it is clear that dielectric properties of NBR matrix gets highly modified by addition of PPy and F-PPy, and the required dielectric constant can be achieved by varying their concentration.

Dielectric loss

The dielectric loss (ε'') is a measure of energy dissipated in the dielectric in unit time when an electric field acts on it. The increased mobility of charge carriers results in an increase in the dielectric loss.[50] While the conducting polymers increase the conductivity of a composite and thereby the dielectric permittivity, they can also impart high dielectric loss. Therefore, ε'' tends to be higher in materials with high ε' value. Loading-dependence of ε'' of PPy-filled and F-PPy-filled NBR composites in S-band frequencies is depicted in Figures 13 and 14, respectively. Dielectric loss is found to increase with PPy

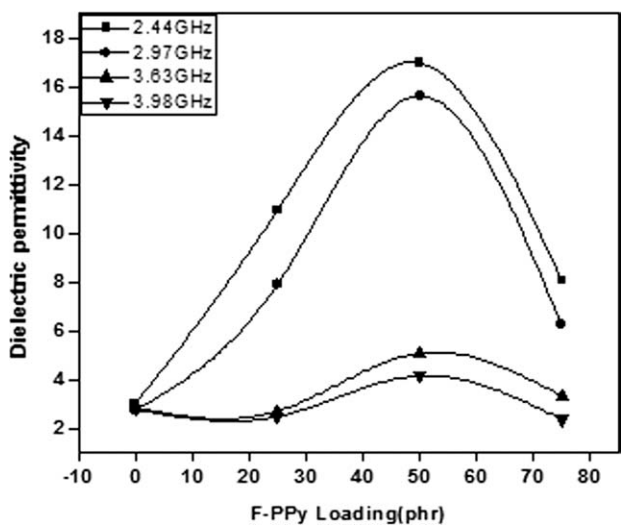

Figure 12 Dielectric permittivity versus F-PPy loading of BFp series.

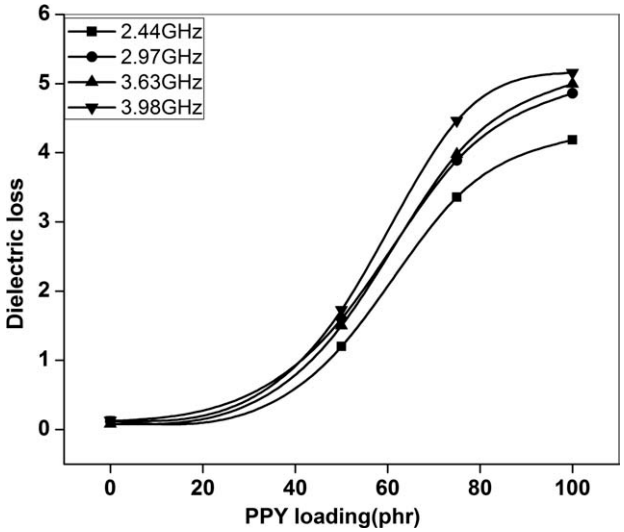

Figure 13 Dielectric loss versus PPy loading of BP series.

loading due to increased mobility of charge carriers while frequency has little effect on ε″ except at higher loading. In the case of BFp series, dielectric loss increases with loading, reaches a maximum at 50 phr loading and then decreases.

AC conductivity

The microwave conductivity is a direct function of dielectric loss and hence the Figures 15 and 16, showing the variation of the AC conductivity (S m^{-1}) of composites with PPy and F-PPy loading at different frequencies, have the same nature as that of the dielectric loss factor. Conductivity of the matrix at lowest loading of filler is affected by three parameters viz the intrinsic conductivity of the filler, the shape of the filler, and also the surface tension

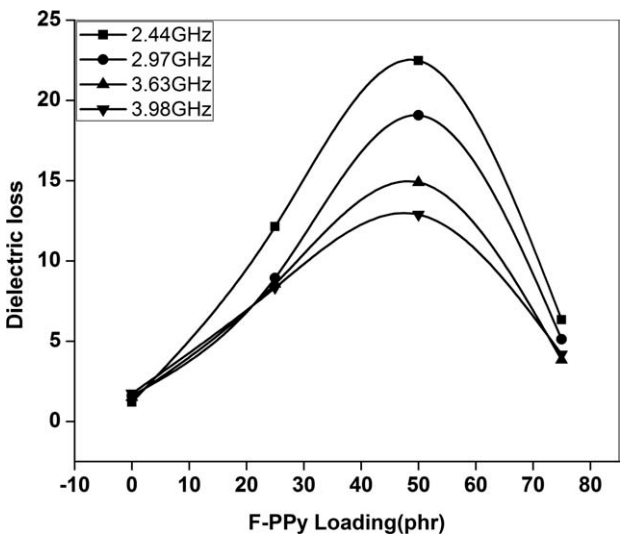

Figure 14 Dielectric loss versus F-PPy loading of BFp series.

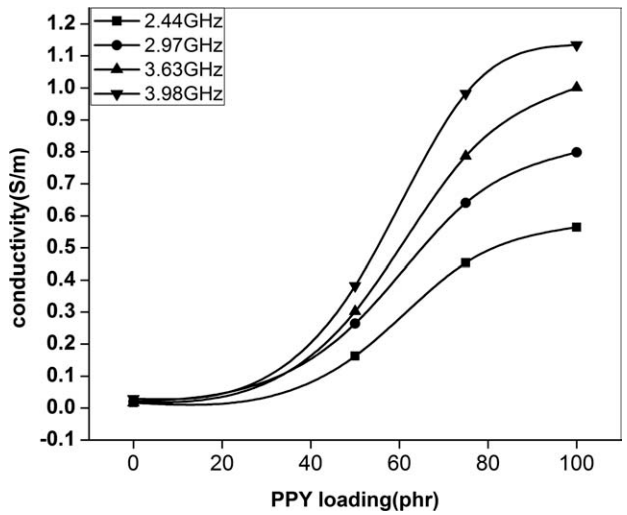

Figure 15 Conductivity versus PPy loading of BP series.

of the matrix and filler.[53] It is expected that fibrous fillers will yield a percolation threshold at lower loadings compared with irregularly shaped particles, as the former will afford many more interparticle contacts. This is the reason for lower threshold and higher AC conductivity of fiber-filled composites. Maximum conductivity 3.1 S m^{-1} is obtained at 50-phr F-PPy-loaded sample at a frequency 2.97 GHz.

Absorption coefficient

As the absorption coefficient is derived from the complex permittivity and is a measure of propagation and absorption of electromagnetic waves when it passes through the medium, the dielectric materials can be classified in terms of this parameter indicating transparency of waves passing through it.[25] The microwave conductivity and absorption

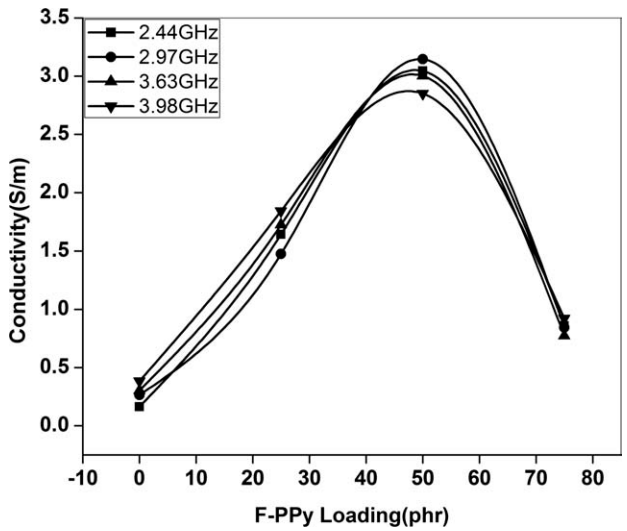

Figure 16 Conductivity versus F-PPy loading of BFp series.

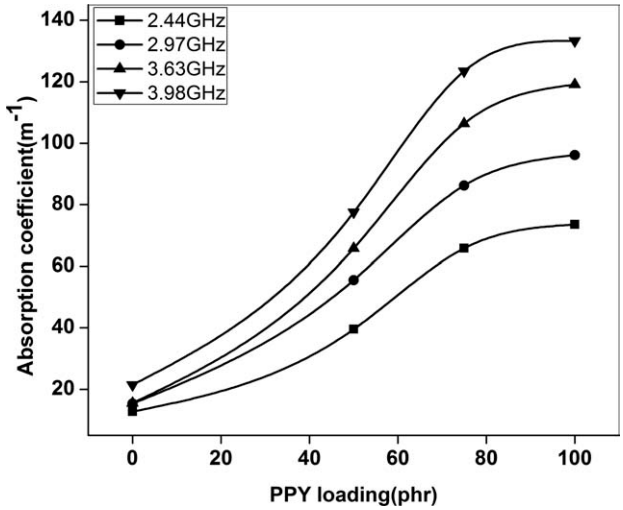

Figure 17 Absorption coefficient versus PPy loading of BP series.

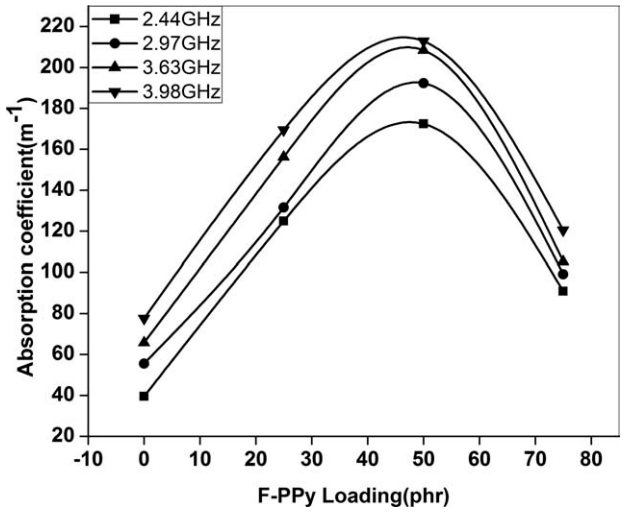

Figure 18 Absorption coefficient versus F-PPy loading of BFp series.

coefficient are direct functions of dielectric loss. The variation of absorption coefficient with frequency and filler loading is same as that for AC conductivity as is evident from Figures 17 and 18. It is clear that the absorption coefficient increases with increase in frequency and also with filler loading and maximum absorption coefficient value is obtained for 50-phr F-PPy-loaded composite.

Dielectric heating coefficient

Table IV shows the variation of dielectric heating coefficient (J) with frequency and with loading. It is observed that the heating coefficient decreases with frequency and also with filler loading. The heat developed is proportional to both frequency and the product of ε and tan δ. Higher the *J* value poorer will be the polymer for dielectric heating purpose. In the present study, *J* value is found to be the lowest for 50-phr F-PPy-loaded sample.

Skin depth

As the skin depth also called the penetration depth, is basically the effective distance of penetration of an electromagnetic wave into the material,[26] it can be applied to a conductor carrying high-frequency signals. The self-inductance of the conductor effectively limits the conduction of the signal to its outer shell and the shells thickness is the skin depth which decreases with increase in frequency. From Table IV, it is clear that the lowest value of skin depth is for the 50-phr F-PPy-loaded NBR.

CONCLUSIONS

The cure characteristics, DC conductivity, mechanical, thermal, and microwave properties of nitrile rubber/PPy and nitrile rubber/PPy-coated short nylon fiber composites were investigated. Cure time increases with the incorporation of PPy, reaches a maximum and then decreases at higher loading, whereas fiber loading decreases the cure time significantly. Compared to PPy, PPy-coated fiber is found to be very effective in enhancing the DC conductivity of NBR. Conductivity of 75-phr PPy-loaded sample is attained by the addition of only 25-phr PPy-coated fiber. Both PPy and PPy-coated fiber are very effective in improving the mechanical

TABLE IV
Dielectric Properties of the Composites in S-Band Frequencies (2–4 GHz)

	Skin depth (m)				Di electric heating coefficient (*J*)			
Composite	2.438 (GHz)	2.972 (GHz)	3.626 (GHz)	3.981 (GHz)	2.438 (GHz)	2.972 (GHz)	3.626 (GHz)	3.981 (GHz)
BP0	0.079	0.065	0.065	0.047	8.064	8.210	12.048	7.581
BP2	0.025	0.018	0.015	0.013	0.832	0.624	0.666	0.578
BP3	0.015	0.012	0.009	0.008	0.298	0.257	0.251	0.224
BP4	0.014	0.010	0.008	0.007	0.239	0.206	0.200	0.194
BFp2	0.008	0.008	0.006	0.006	0.082	0.112	0.117	0.120
BFp3	0.006	0.005	0.005	0.005	0.045	0.052	0.067	0.078
BFp4	0.011	0.010	0.009	0.008	0.158	0.195	0.261	0.240

properties of NBR. Incorporation of PPy and PPy coated improve the thermal stability of NBR. The dielectric permittivity of the conducting composites prepared is much greater than the gum vulcanizate. Dielectric constant as high as 43 is obtained for 75-phr PPy-loaded sample at 3.9 GHz frequency. The composites exhibit much higher AC conductivity compared to gum vulcanizate and the maximum of 3.1 S m^{-1} is obtained for 50-phr fiber-loaded sample. The conducting composites prepared show substantial improvement in other microwave properties such as dielectric heating coefficient, skin depth, and absorption coefficient.

References

1. Achour, M. E.; Brosseau, C., Eds. Prospects in Filled Polymers Engineering: Mesostructure, Elasticity Network, and Macroscopic Properties; Transworld Research Network, Singapore, 2008; p. 129.
2. Achour, M. E.; Brosseau, C.; Carmona, F. J Appl Phys 2008, 103, 9.
3. Bryning, M. B.; Islam, M. F.; Kikkawa, J. M.; Yodh, A. G. Adv Mater 2005, 17, 1186.
4. Bohwon, K.; Koncar, V.; Devaux, E.; Dufour, C.; Vialllier, P. Synth Met 2004, 146, 167.
5. Hansen, T. S.; West, K.; Hassager, O.; Larsen, N. B. Synth Met 2006, 156, 1203.
6. Soares, B. G.; Amorim, G. S.; Souza, F. G., Jr.; Oliveira, M. G.; Silva, J. E. P. Synth Met 2006, 156, 91.
7. Faez, R.; Schuster, R. H.; De Paoli, M .A. Eur Polym J 2002, 38, 2459.
8. Moreira, V. X.; Garcia, F. G.; Soares, B. G. J Appl Polym Sci 2006, 100, 4059.
9. Koops, C. G. Phys Rev 1951, 83, 121.
10. Brockman, F. G.; Matteson, K. E. J Am Ceram Soc 1971, 54, 183.
11. Jankowski, S. J Am Ceram Soc 1988, 71, C46.
12. Gangopadhyay, R.; De, A. Chem Mater 2000, 12, 608.
13. Achour, M. E.; Droussi, A.; Zoulef, S.; Gmati, F.; Fattoum, A.; Belhadj Mohamed, A.; Zangar, H. Spectrosc Lett 2008, 41, 299.
14. Shin, H. W.; Lee, J. Y.; Heum, Y. Mol Cryst Liq Cryst 2008, 492, 403.
15. Kim, H. K.; Kim, M. S.; Chun, S. Y. Mol Cryst Liq Cryst 2003, 405, 161.
16. Jamadade, S.; Jadhav, S.; Puri, V. Arch Phys Res 2010, 1, 205.
17. Hong-Quan, X.; Cheng-Mei, L.; Jun-Shi, G. Polym Int 1999, 48, 1099.
18. Neoh, K. G.; Tay, B. K.; Kang, E. T. Polymer 2000, 41, 9.
19. Goettler, L. A.; Shen, K. S. Rubber Chem Technol 1983, 56, 619.
20. Setue, D. K.; De, S. K. J Mater Sci 1984, 19, 983.
21. Saritha, C. A., Ph.D. Thesis, Cochin University of Science and Technology, India, 2008.
22. Kupfer, K.; Kraszewski, A.; Knoochel, R. Sensors Update; Wiley-VCH: Weinheim, 2000, 7, 186.
23. Ku, C. C.; Liepins, R. Electrical Properties of Polymers: Chemical Principles; Hansen Publishers: Munich, 1987; p. 92.
24. Ezquerra, T. A.; Kremmer, F.; Wegner, G. Prog Electromagn Res 1992, 6.
25. Bradford, L. S.; Carpentier, M. H. The Microwave Engineering Hand Book; Chapman & Hall: London, 1993.
26. Stephen, C. W.; Frederic, H. L. Microwaves Made Simple: Principles and Applications; United States Book crafters: Chelsea, 1985.
27. Kassim, A.; Mahmud, H. N. M.; Yee, L. M.; Hanipah, N. Pacific J Sci Technol 2006, 7, 103.
28. Rasika Dias, H. V.; Fianchini, M.; Gamini Rajapakse, R. M. Polymer 2006, 47, 7349.
29. Shiigi, H.; Kishimoto, M.; Yakabe, H.; Deore, B.; Nagaoka, J. Anal Sci 2002, 18, 41.
30. Davidson, R. G.; Turner, T. G. Synth Met 1996, 79, 165.
31. Chen, W.; Xingwei, L.; Gi, X.; Zhaoquang, W.; Wenquing, Z. Appl Surf Sci 2003, 218, 216.
32. Varesanoa, A.; Aluigia, A.; Florio, L.; Riccardo, F. Synth Met 2009, 159, 1082.
33. Sreeja, T. D.; Kutty, S. K. N. Polym Plast Technol Eng 2003, 42, 239.
34. Seema, A.; Kutty, S. K. N. J Appl Polym Sci 2006, 99, 532.
35. Kim, D. K.; Oh, K. W.; Ahn, H. J.; Hun, S. K. J Appl Polym Sci 2008, 107, 3925.
36. Taunk, M.; Atul Kapil, A.; Chan, S. Solid State Commun 2010, 150, 1766.
37. Varesano, A.; Tonin, C.; Ferrero, F.; Stringhetta, M. J Thermal Anal Calorim 2008, 94, 559.
38. Kaynak, A.; Beltran, R. Polym Int 2003, 52, 1021.
39. Kelly, F. M.; Johnston, H. J.; Borrmann, T.; Richardson, M. J. 2007, DOI: 10.1002/ejic.200700608.
40. Cucchi, I.; Boschi, A.; Arosiob, C.; Bertini, F.; Freddib, G.; Catellani, M. Synth Met 2009, 159, 246.
41. Murugendrappa, M. V.; Khasim, M.; Ambika Prasad, M. V. N. Bull Mater Sci 2005, 28, 565.
42. Vishnuvardhan, T K.; Kulkarni, V. R.; Basavaraja, C.; Raghavendra, S. C. Bull Mater Sci 2006, 29, 77.
43. Li, G.; Liao, X.; Sun, X.; Yu, J.; He, J. Front Chem China 2007, 2, 118.
44. Gu, Z.; Zhang, L.; Li, C. J Macromol Sci Part B 2009, 48, 6, 1093.
45. Smirnov, M. A.; Kuryndin, I. S.; Nikitin, L. N.; Sidorovich, A. V.; Yu, N.; Sazanov, O. V.; Kudasheva, V.; Bukošek, A. R.; Khokhlov, N. S.; Elyashevich, G. K. Russ J Appl Chem 2005, 78, 1993.
46. Cataldo, F.; Omastova, M. Polym Degrad Stab 2003, 82, 487.
47. Zoppi, R. A.; De Paoli, M. A. Polymer 1996, 37, 1999.
48. Gilman, J. W. Appl Clay Sci 1999, 15, 31.
49. Abbas, S. M.; Chandra, M.; Verma, R.; Chatterjee, R.; Goel, T. C. Compos A 2006, 37, 2148.
50. Al-Nasrawy, D. K. M. J Electron Dev 2011, 9, 409.
51. Soloman, M. A.; Philip Kurian, M. R.; Anantharaman, P. J Appl Polym Sci 2003, 89, 769.
52. John, H. Ph.D. Thesis, Cochin University of Science and Technology, India, 2003.
53. Skotheim, T. A. Handbook of Conducting Polymers, Marcel Dekker, New York, 1986; Vols 1 and 2.